SCIENCE CHINA
Chemistry

• ARTICLES •
• SPECIAL TOPIC • Highly Branched Polymers–Promising Architectural Macromolecules

December 2010 Vol.53 No.12: 2461–2471
doi: 10.1007/s11426-010-4134-5

Miktoarms hyperbranched polymer brushes: One-step fast synthesis by parallel click chemistry and hierarchical self-assembly

HAN Yi & GAO Chao*

MOE Key Laboratory of Macromolecular Synthesis and Functionalization; Department of Polymer Science and Engineering, Zhejiang University, Hangzhou 310027, China

Received July 25, 2010; accepted August 20, 2010

Spherical molecular brushes with amphiphilic heteroarms were facilely synthesized by grafting the arms of hydrophobic 2-azidoethyle palmitate and hydrophilic monoazide-terminated poly(ethylene glycol) onto the core of alkyne-modified hyperbranched polyglycerol (HPG) with high molecular weight (M_n = 122 kDa) via one-pot parallel click chemistry. The parallel click grafting strategy was demonstrated to be highly efficient (~100%), very fast (~ 2 h) and well controllable to the amphilicity of molecular brushes. Through adjusting the feeding ratio of hydrophobic and hydrophilic arms, a series of brushes with different arm ratios were readily obtained. The resulting miktoarms hyperbranched polymer brushes (HPG-*g*-C16/PEG350) were characterized by hydrogen-nuclear magnetic resonance (^{1}H NMR), Fourier transform infrared (FT-IR) spectroscopy, gel permeation chromatography (GPC), and differential scanning calorimetry (DSC) measurements. The spherical molecular brushes showed high molecular weights up to 230 kDa, and thus could be visualized by atomic force microscopy (AFM). AFM and dynamic laser light scattering (DLS) were employed to investigate the self-assembly properties of amphiphilic molecular brushes with closed proportion of hydrophobic and hydrophilic arms. The brushes could self-assemble hierarchically into spherical micelles, and network-like fibre structures, and again spherical micelles by addition of *n*-hexane into the dichloromethane or chloroform solution of brushes. In addition, this kind of miktoarms polymer brush also showed the ability of dye loading via host-guest encapsulation, which promises the potential application of spherical molecular brushes in supramolecular chemistry.

miktoarms, molecular brushes, hyperbranched polyglycerol, amphiphilic, self-assembly

1 Introduction

Attaching high density polymeric chains/arms with one end to a macromolecular backbone affords a molecular polymer brush [1–2]. Using linear polymers and dendritic/hyperbranched polymers as backbones, cylindrical/bottle and spherical molecular brushes can be constructed, respectively. Numerous papers have been published on the molecular brushes during the last few decades [2–5]. One of the most important reasons is that the architecture of molecular brushes is well-known in biology, and such architecture is responsible for various functions including mucociliary clearance of lung airways and mechanical performance of articular cartilage [2]. From this point of view, molecular brushes offer us a good opportunity to access biomimetic polymers. Besides, molecular brushes can also be used as single molecular templates for inorganic nanoparticles formation and they also have potential application in fields of solubilizer, catalysis and drug delivery [6–10].

Recently, miktoarms molecular brushes (MMBs) are of particular interest because their dynamic assembly nature associated with the complicated molecular structure may have significantly further use in biomimetics field [3]. MMBs are generally synthesized by tandem multi-pot grafting strategy via combination of different controlled/

*Corresponding author (email: chaogao@zju.edu.cn)

living radical polymerizations [11–17]. For instance, Huang and coworkers synthesized HPG-*graft*-PAA/PS through the combination of atom transfer radical polymerization (ATRP) and reversible addition-fragmentation chain transfer (RAFT) polymerization [18]. Matyjaszewski *et al*. successfully prepared many kinds of molecular brushes by using controlled/living radical polymerization and "click" chemistry [19–21]. In their work, grafting from, grafting to and grafting through strategies were frequently applied synchronously. Yan and Pan synthesized a dendritic heteroarm star copolymer that contains multi-alternating arms of poly(ethyleneoxide-tetrahydrofuran) (P(EO-THF)) and poly(methyl methacrylate) (PMMA) on a dendritic polyester core. They applied "core-first" approach by combination of sequential cationic ring-opening polymerization (CROP) and RAFT polymerization initiated by a dendritic macroinitiator [22]. Such a tandem multi-pot grafting strategy enables complex macromolecular structures available, putting significant advancements for molecular brushes. However, its drawbacks are emerging gradually with the development of this field: (1) the multistep synthesis process is laborious and troublesome, always leading to low yield of final product and thus posing an obstacle for the deep research on the structure-property relationship and application of MMBs; (2) the grafting efficiency of the later step is normally lower than that of the first grafting step due to the steric hindrance of grafted arms; (3) the molecular parameters such as degree of polymerization and PDI of grafted arms are difficult to be measured. Hence, more convenient and powerful strategy is eagerly expected. Recently, enlightened by the orthogonal organic reaction [23], Gao *et al.* presented the novel "one-pot orthogonal multigrafting" strategy for synthesis of amphiphilic MMBs by the combination of ATRP 'grafting from' and azide-alkyne click chemistry 'grafting to' in one pot [3], opening an avenue to facile preparation of desired macromolecules with tailor-made structures. Most recently, Gao and coworker presented a "one-step parallel multigrafting" approach to synthesis of miktoarms sliding supramolecular brushes [24]. This parallel grafting method allows different side chains could be attached to the same anchoring group of backbone simultaneously, facilitating the synthesis of well-defined miktoarms brushes with tunable properties. Herein, we extend the parallel strategy from the backbone of supramolecular polyrotaxane to hyperbranched polymer for the convenient construction of miktoarms hyperbranched polymer brushes (MHPBs).

Our synthesis protocol was displayed in Scheme 1. We chose high molecular weight hyperbranched polyglycerol (HPG) as the core because HPG with narrow polydispersity and high molecular weight could be obtained via anionic ring-opening polymerization of glycidol [25–27] and it has been proved biocompatible [28–30]. Besides, HPG is a typical kind of hydrophilic hyperbranched polymer rich of hydroxyl end groups which can be converted into various desired functional end groups through appropriate transformation, especially esterification reaction. Low grafting efficiency had always been a problem for the "grafting to" route because of the steric hindrance of the side chains and the low reactivity for the coupling reaction [18]. To meet this challenge, two important points were considered in our

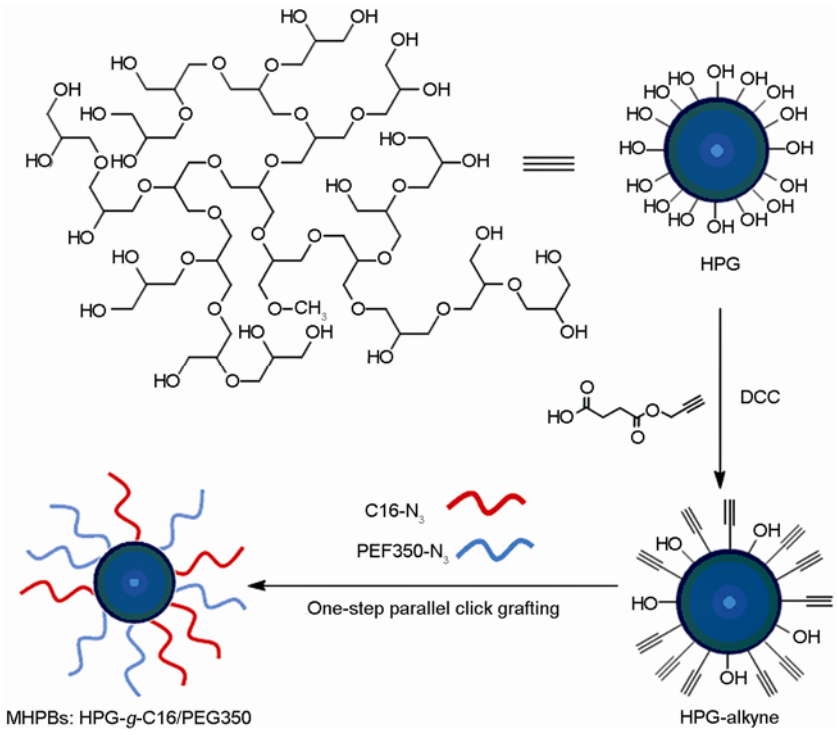

Scheme 1 The protocol for synthesizing miktoarms hyperbranched polymer brushes (MHPBs) of HPG-*g*-C16/PEG350 via one-step parallel click grafting strategy.

molecular design. On one hand, some relatively "soft" and "thin" chains such as low molecular weight of poly(ethylene glycol) (PEG) and palmitic acid (C16) were picked as the side chains in order to weaken the steric hindrance [20]. On the other hand, we employed the Cu(I)-catalyzed 1,3-dipolar cycloaddition reaction between azide and alkyne, named "click" chemistry [31], to immobilize the side chains due to its merits of high reactivity, good specificity and nearly quantitative yield. Recent years have witnessed the rapid development of click chemistry, through which libraries of functional molecules, polymers, biomacromolecules, and nanosurfaces have been constructed facilely [32]. As a consequence, we successfully synthesized MHPBs via the one-step click parallel grafting strategy with extremely high efficiencies (~100%).

Miktoarms brushes always have interesting self-assembly behaviors [33]. The self-assembly of miktoarms cylindrical brushes has been intensively investigated, while that of MHPBs with spherical topology is still in infancy [34–36]. Yan and coworkers synthesized a kind of amphiphilic macromolecules with a hydrophobic hyperbranched poly(3-ethyl-3-oxetanemethanol) core (HBPO) and many hydrophilic PEG arms, which could self-assemble into macroscopic multiwalled tubes millimeters in diameter and centimeters in length, opening the two directions of macroscopic molecular self-assembly and supramolecular self-assembly of irregular macromolecules [35, 37]. Brooks and coworkers synthesized mixed arm star copolymers of poly(*N,N*-dimethylacrylamide) (PDMA) and poly(*N-iso*-propylacrylamide) (PNIPAm) and found micelle-like structures in their system [38]. Recently, our group found that MHPBs could show hierarchical self-assembly behavior [3]. In this article, we also investigated the self-assembly behaviors of our MHPBs, HPG-*g*-C16/PEG350. Interestingly, hierarchical self-assembly morphologies were also observed in the experiments.

2 Experimental

2.1 Materials

HPG (M_n = 122 kDa, PDI = 1.16, DP = 1650), 2-azidoethanol, 4-oxo-4-(prop-2-ynyloxy)butanoic acid and 4-(2-azido-ethoxy)-4-oxobutanoic acid were synthesized according to the previous work of our group [39, 40]. CuBr (purified according to ref. [21] before use, 98%) were purchased from Sigma–Aldrich. 4-(Dimethylamino) pyridine (DMAP, 99%), poly(ethylene glycol) monomethyl ether (M_n = 350 Da, PEG350) and 1,1,4,7,7-pentamethyl-diethylenetriamine (PMDETA, 98%) were all purchased from Alfa Aesar. *N,N′*-Dicyclohexylcarbodimide (DCC, 98%) was obtained from GL Biochem Shanghai Ltd. All the other raw materials of reagents were purchased from Aldrich and were used as received except for those specially mentioned. All solvents were used as received without further purification except for those specially mentioned.

2.2 Characterization

Hydrogen-nuclear magnetic resonance (^{1}H NMR) measurements were conducted on a Varian Mercury 400 MHz spectrometer using $CDCl_3$ as the solvent. The molecular weights of the polymers were measured on PE Series 200 gel permeation chromatography (GPC) with polystyrene as the standards and using LiBr/DMF (0.01 mol/L) as the eluent at a flow rate of 1 mL/min. A PE Paragon 1000 spectrometer was applied to record Fourier transform infrared (FT-IR) spectra using KBr disks. Dynamic laser light scattering (DLS) measurements were carried out on a BI-200SM Dynamic/static Laser Light Scattering, Brookhaven, and the wavelength of the laser is 630 nm. AFM images were conducted with a Digital Instrument (DI) Nanoscope IIIa scanning probe microscope, under tapping mode. Differential scanning calorimetry (DSC) measure- ments were carried out on a DSCQ200 with a scanning rate at ±15 °C per minute, and the scanning range was from –60 to 150 °C, and the whole scanning process contained two heating and one cooling scans.

2.3 Synthesis of alkyne-modified HPG (HPG-alkyne)

HPG (0.395 g, 5.34 mmol hydroxyl) and *N,N*-dimethylformamide (DMF, 2 mL) were added into a Schlenk flask under nitrogen flow and stirred until the HPG was totally resolved and the flask was immerged into the ice-water bath. Then *N,N*-dicyclohexylcarbodimide (DCC, 0.771 g, 3.74 mmol), 4-oxo-4-(prop-2-ynyloxy)butanoic acid (designated as alkyne-COOH, 0.583 g, 3.74 mmol), and 4-(dimethylamino)pyridine (DMAP, 0.0456 g, 0.37 mmol) were added into the reaction system and the flask sealed was with a rubber plug. The reaction was carried out in darkness for 24 h at room temperature. During the reaction, a small amount of dichloromethane was added when the system became too viscous. Then the mixture was filtered and the residual dichloromethane removed by a rotary evaporator under reduced pressure. After that, the mixture was precipitated in de-ionized water followed by solubilizing the precipitate with acetone as little as possible and then filtered. The solution was precipitated in de-ionized water twice. The final product (designated as HPG-alkyne) was obtained after drying in a vacuum oven overnight at 30 °C (0.285 g, yield 20.3%). The final product was light yellow and sticky and should be stored in the dark.

2.4 Synthesis of azide-modified palmitic acid (C16-N_3)

To the Schlenk flask DCC (9.08 g, 0.044 mol), dichloromethane (20 mL), palmitic acid (6.96 g, 0.044 mol), 2-azidoethanol (6.96 g, 0.088 mol) and DMAP (0.538 g,

0.0044 mol) were added under nitrogen flow and the mixture was stirred with a magnetic bar. The flask was immerged in an ice-water bath and the reaction lasted for 24 h in darkness after sealing the system. Then the mixture was filtered and the filtrate was washed by hydrochloric acid (1 M) for 3 times and then de-ionized water for 3 times and then NaOH solution (1 M) for 3 times and again de-ionized water for 3 times. At last, the solvent was removed by a rotary evaporator under reduced pressure. The final product (designated as C16-N_3) was obtained after being dried in the vacuum oven at room temperature over night (9.48 g, yield 72.9%).

2.5 Synthesis of monoazide-terminated poly(ethylene glycol) (PEG350-N_3)

For the synthesis of PEG350-N_3 [32], the reaction condition was the same as the synthesis of C16-N_3. PEG350 (10 g, 28.6 mmol hydroxyl), 4-(2-azidoethoxy)-4-oxobutanoic acid (designated as N_3-COOH, 6.414 g, 34.3 mmol), dichloromethane (130 mL), DCC (7.076 g, 34.3 mmol), and DMAP (0.419 g, 34.3 mmol) were added to the Schlenk flask under nitrogen flow. After the reaction, the mixture was filtered and the filtrate was washed by the hydrochloric acid (1 mol/L) for 4 times, de-ionized water once, NaOH solution (1 mol/L) twice and again de-ionized water once. Then the solution was dried by anhydrous magnesium sulfate overnight. After that, the solvent was removed by a rotary evaporator under reduced pressure. The final product (designated as PEG350-N_3) was obtained after dried in the vacuum oven at room temperature over night (13.00 g, yield 75.7%).

2.6 Synthesis of miktoarms polymer brushes (HPG-*g*-C16/PEG350)

Six samples of brushes with the content of C16 arms varied from 0 to 100% were synthesized [24]. We take the HPG-C16(50)-PEG350(50) as an example (the number in the parenthesis indicated the molar feed ratio) to illustrate the synthesis details. To the Schlenk flask HPG-alkyne (20.0 mg, 0.0618 mmol of alkyne groups calculated by the ^{1}H NMR spectrum), C16-N_3 (20.1 mg, 0.0618 mmol), PEG350-N_3 (32.07 mg, 0.0618 mmol), dichloromethane (4 mL) were added and the flask was deoxygenated by bubbling nitrogen for 10 min. Then CuBr (1.77 mg, 0.0124 mmol) and PMDETA (2.61 μL, 0.0124 mmol) were added to the flask under nitrogen flow. The reaction was carried out under room temperature and lasted for 2 h in darkness. After the reaction, the mixture was precipitated in the methanol for three times. The final product of HPG-C16(50)-PEG350(50) was obtained after dried in a vacuum oven at room temperature overnight. It must be noted that HPG-C16(0)-PEG350(100), HPG-C16(25)-PEG350(75) and HPG-C16(100)-PEG350(0) were precipitated in ether to get a higher yield because of their different solubility.

2.7 Self-assembly of the miktoarms polymer brushes

To investigate the self-assembly process and the supramolecular structure of the miktoarms polymer brushes, we firstly prepared different polymer solutions with different solvent and different initial concentrations. Dichloromethane and chloroform (both were newly distilled) were chosen as the solvent and the initial concentration was 1, 0.5 and 0.25 mg/mL, respectively. After the polymers were totally resolved overnight, a certain amount of *n*-hexane (newly distilled) was added into the solution until white turbidity appears. After keeping the samples still for at least half an hour, the hydrodynamics radius (R_h) of the self-assembly structure was measured by DLS at 25 °C [41], followed by making the self-assembly samples by the spin-coating method on freshly-peeled mica substrates for AFM measurements afterwards.

2.8 Dye loading of the miktoarms polymer brushes (HPG-*g*-C16/PEG350)

To investigate the dye loading ability of HPG-*g*-C16/PEG350, we prepared three sorts of solution, and they were HPG-C16(36)-PEG350(64) in dichloromethane, HPG-C16(36)-PEG350(64) in chloroform and HPG-C16(100)-PEG350(0) in dichloromethane respectively with the same concentration of 3 mg/mL. A certain amount of Congo red aqueous solution was added into the polymer solution and then shaken the bottle fiercely. Then the bottles were kept still for about 12 h to be compared with the blank samples.

3 Results and discussion

3.1 Design and synthesis of alkyne modified HPG (HPG-alkyne)

Scheme 1 depicts the protocol for synthesis of the MHPBs. In order to graft C16-N_3 and PEG350-N_3 to the HPG core via "click" reaction, HPG-alkyne was synthesized at first. A typical DCC/DMAP condensation reaction between alkyne-COOH and multihydroxyl HPG was applied in this case. Figure 1 (a) and Figure 2(c) show the ^{1}H NMR and FT-IR spectra of HGP-alkyne. All the peaks in the ^{1}H NMR spectrum were labeled by letters corresponding to the protons of the products. Compared with pristine HPG [26–27], two main new peaks appeared in the ^{1}H NMR spectrum of HPG-alkyne: peak b (OCH_2CCH) at 5.18 ppm and peak c (CH_2CH_2COO) at 2.67 ppm, indicating the successful linkage of alkyne and HPG. Because $CDCl_3$ is not a good solvent for HPG, and the terminal chains have the shielding effect, the peaks of protons of HPG core are slightly weakened. Calculated from the ^{1}H NMR spectrum, ~ 40% of hydroxyl groups of HPG were modified by alkyne moieties.

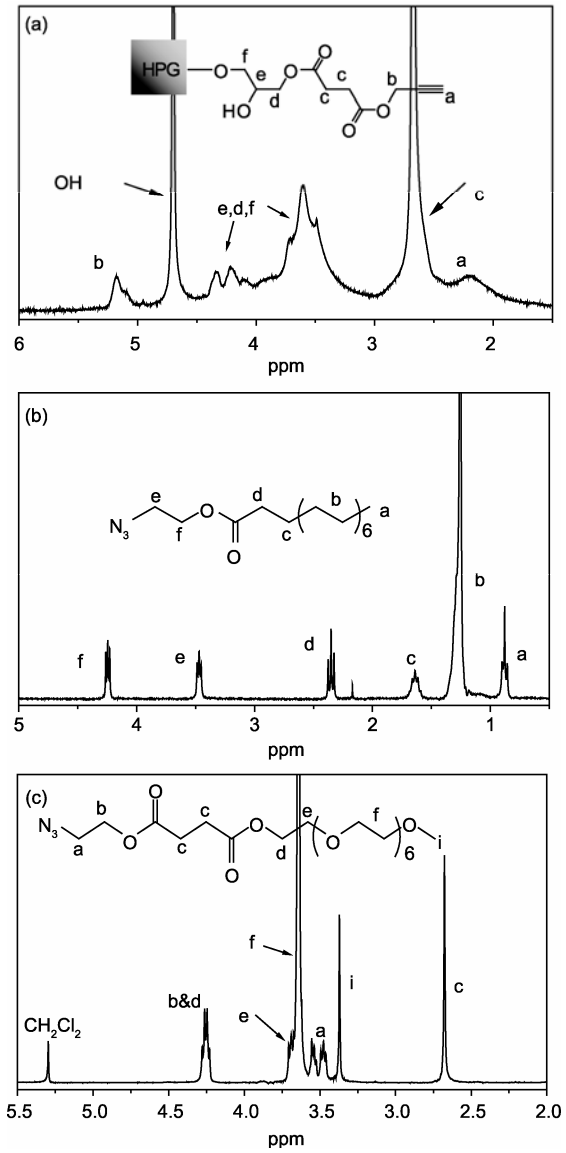

Figure 1 ^{1}H NMR spectra of (a) HPG-alkyne, (b) azide-modified palmitic acid and (c) monoazide-terminated poly(ethylene glycol) in $CDCl_3$.

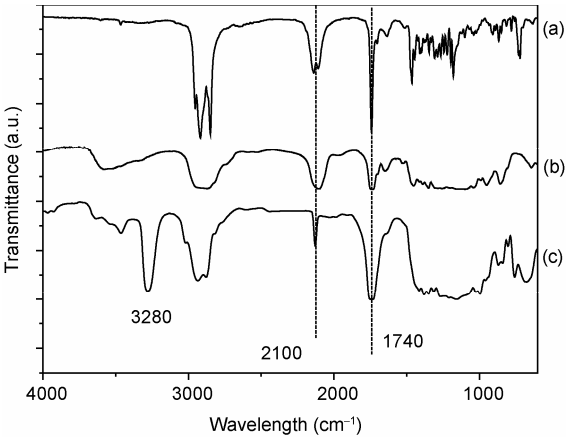

Figure 2 FT-IR spectra of azide-modified palmitic acid (a), monoazide-terminated poly(ethylene glycol) (b) and HPG-alkyne (c).

Since the degree of polymerization (DP) of HPG is about 1650, around 660 hydroxyl groups were converted into alkyne groups. From the FT-IR spectrum (Figure 2), the absorption peaks of alkyne groups around 2100 and 3280 cm^{-1} and the peak of carbonyl groups around 1740 cm^{-1} can be clearly identified, confirming the formation of the expected structure.

3.2 Synthesis of azide-modified palmitic acid (C16-N_3) and monoazide-terminated poly(ethylene glycol) (PEG350-N_3)

Low grafting efficiency and poor controllability were the main drawbacks of the "grafting onto" strategy. Nevertheless, Matyjaszewski and coworkers reported that click "grafting onto" could also work well in the synthesis of molecular brushes, if the flexible grafts like PEG were employed [20]. In order to increase the grafting efficiency, we chose C16 as the hydrophobic arms because they are also "soft" and "thin". The side arm of C16-N_3 was also synthesized via the classic DCC/DMAP condensation reaction between palmitic acid and 2-azidoethanol. From the ^{1}H NMR spectrum of C16-N_3 (Figure 1(b)), the corresponding hydrogen peaks are clearly found, particularly for the peak f ($OCH_2CH_2N_3$) at 4.24 ppm, peak e ($OCH_2CH_2N_3$) at 3.48 ppm and peak d (CH_2COO) at 2.35 ppm, demonstrating the successful condensation between the two materials. In the FT-IR spectrum of C16-N_3 (Figure 2(a)), the peak of azido groups around 2100 cm^{-1} and the peak of carbonyl groups at 1740 cm^{-1} further clarified the product structure.

Likewise, another "soft" chain, PEG350-N_3 was synthesized and also confirmed by ^{1}H-NMR and FT-IR spectra, as shown in Figure 1(c) and Figure 2(b).

3.3 Synthesis and characterization of miktoarms polymer brushes (HPG-*g*-C16/PEG350)

Miktoarms brushes of HPG-*g*-C16/PEG350 were synthesized by parallel "click" reaction between HPG-alkyne and azide terminated arms (i.e., C16-N_3 and PEG350-N_3). To tune the amphiphilicity of molecular brushes, we changed the feed fraction of C16-N_3 to PEG350-N_3 (R_{feed}) from 0/100 to 100/0 so that brushes with different arm proportions could be obtained. Their chemical structures were all characterized by FT-IR and ^{1}H NMR spectra (Figure 3). In Figure 3 (a), the absorption peak around 2100 cm^{-1} can be hardly seen. This indicated that the degree of "click" coupling reaction was near 100% and no residual C16-N_3 and PEG350-N_3 could be detected, since both azido and alkyne groups have sharp absorption around 2100 cm^{-1}. Another advantage of "click" reaction is the high stability of triazole ring. In addition, the "click" grafting could be completed in two hours, which was much faster than the "grafting from" methods reported.

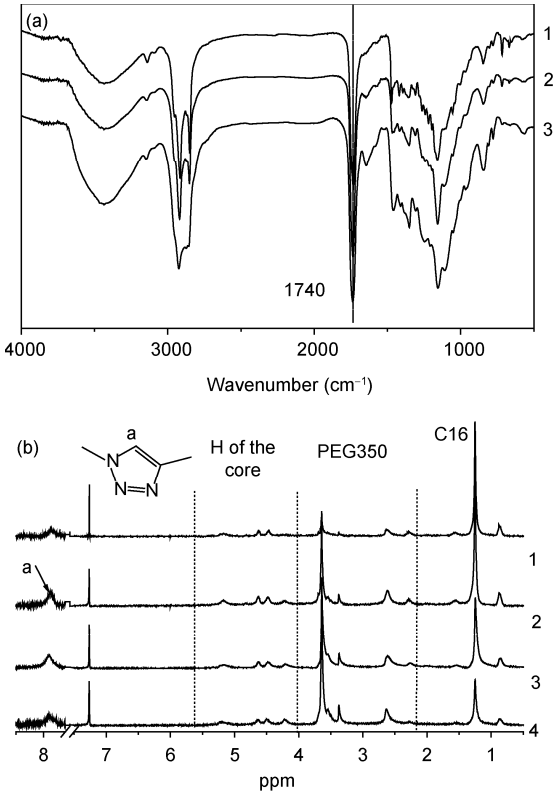

Figure 3 (a) FT-IR spectra of HPG-*g*-C16/PEG350 with different arms ratios: (1) HPG-C16(75)-PEG350(25), (2) HPG-C16(50)-PEG350(50), (3) HPG-C16(25)-PEG350(75) and (b) ^{1}H-NMR spectra in $CDCl_3$: (1) HPG-C16(75)-PEG350(25), (2) HPG-C16(50)-PEG350(50), (3) HPG-C16(36)-PEG350(64), (4) HPG-C16(25)-PEG350(75). The left part of (b) is enlarged by 7 times to make the peak of the triazole ring at 7.87 ppm more clear.

In Figure 3(b), the peak around 7.87 ppm can be assigned to the triazole ring after "click" reaction, and the peaks at 3.59–3.64 ppm and 1.14–1.32 ppm the protons of the PEG arms and C16 arms, respectively, and the peaks ranged from 4.1 to 4.5 ppm the protons of the core. The actual arms fraction of the final brushes (R_{brush}) can be calculated from the corresponding ^{1}H NMR signals. In order to improve the grafting efficiency, excess of azide group-terminated arms were added, twice as many as alkyne groups. Notably, the purification process is quite simple because the excessive C16-N_3 and PEG350-N_3 could be washed away completely in a proper solvent which is the precipitator of the polymer brushes.

According to the previous work of our group [24], C16-N_3 and PEG350-N_3 can be efficiently attached to the core and should have comparable reactivity in click coupling. These two factors make it possible to get polymer brushes with uniform R_{brush} and tune the R_{brush} by R_{feed}. The values of R_{feed} and R_{brush} are listed in Table 1. It is found that R_{brush} increases regularly with increasing the R_{feed}, indicating the arm fraction or amphiphilicity of brushes can be tuned easily by the feed fraction of two arms. This conclusion also shows the major advantage of the parallel grafting strategy

Table 1 Feed ratios of C16-N_3/PEG350-N_3 and arms ratios of C16/PEG350 of final products for all samples

Sample	R_{feed} [a)]	R_{brush} [b)]
HPG-C16(0)-PEG350(100)	0/100	0/100
HPG-C16(25)-PEG350(75)	25/75	38/62
HPG-C16(36)-PEG350(64)	36/64	52/48
HPG-C16(50)-PEG350(50)	50/50	64/36
HPG-C16(75)-PEG350(25)	75/25	84/16
HPG-C16(100)-PEG350(0)	100/0	100/0

a) Feed ratio of C16-N3/PEG350-N3 in the click coupling reaction. b) Arms ratio of C16/PEG350 calculated from the corresponding ^{1}H NMR spectrum.

since it is hard to vary the side chain ratios in the conventional tandem grafting methods. In addition, we can also find that the R_{brush} is slightly greater than R_{feed} for the miktoarm brushes, which is likely attributed to the two reasons of a little higher reactivity for C16-N_3 and the relatively higher integration for C16-N_3 signals in ^{1}H NMR spectrum owing to the slightly better solubility of C16 chains in $CDCl_3$. The previous work also demonstrated that $CDCl_3$ is the best solvent as far as we know, and the integration error caused by the tiny solubility difference could be safely neglected [24].

Gel permeation chromatography (GPC) was also used to track the molecular weight changes from HPG to brushes of HPG-*g*-C16/PEG350, and the results were shown in Figure 4 and listed in Table 2. In the GPC elution curves (Figure 4), monodispersed peak is observed for HPG-alkyne core, whereas relatively broad peak with a shoulder was observed for each sample of brushes. The shoulder peak may be caused by the polydispersity of the amphiphilic brushes. The number-average molecular weight (M_n) increased apparently after the modification on HPG. In Table 2, both the molecular weights measured by GPC and calculated from ^{1}H NMR spectra were listed. Because the hydrodynamic volume of the spherical hyperbranched polymer brushes was much smaller than that of linear polymer standards, the molecular weights measured by GPC would be smaller than

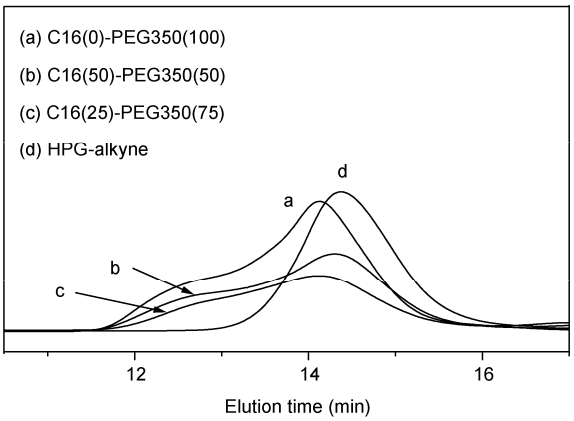

Figure 4 GPC curves of HPG-alkyne and brushes of HPG-*g*-C16/PEG350.

Table 2 Molecular weights of HPG, HPG-alkyne, and brushes HPG-*g*-C16/PEG obtained by GPC and ^{1}H-NMR measurements

Samples [a]	M_p [b]	M_w [c]	M_n [d]	PDI [e]	M_{NMR} [f]	$R_{NMR/GPC}$ [g]
HPG	1.516e+005	1.426e+005	1.222e+005	1.16	—	—
HPG-alkyne	1.782e+005	1.815e+005	1.415e+005	1.28	2.097e+005	1.482
HPG-C16(0)-PEG(100)	2.243e+005	4.248e+005	2.388e+005	1.78	5.470e+005	2.291
HPG-C16(25)-PEG(75)	2.260e+005	3.977e+005	2.331e+005	1.70	4.991e+005	2.141
HPG-C16(50)-PEG(50)	1.903e+005	4.032e+005	2.147e+005	1.88	4.663e+005	2.172

a) GPC results for HPG-C16(75)-PEG(25) and HPG-C16(100)-PEG(0) are not listed because they are not well dissolved in DMF. b) Peak molecular weight measured by GPC. c) Weight-average molecular weight measured by GPC. d) Number-average molecular weight measured by GPC. e) Polydispersity index of the polymers measured by GPC. f) Calculated molecular weight from the ^{1}H-NMR spectrum. g) The ratio of molecular weight calculated from ^{1}H NMR to number-average molecular weight obtained from GPC.

the real ones. The molecular weight calculated from the ^{1}H-NMR spectrum (M_{NMR}) is obviously higher than the corresponding GPC-measured value. Considering the shielding effect of core in the NMR measurements, the M_{NMR}s should be higher than the real ones. So the real M_n for the brushes would be in between M_{GPC} and M_{NMR}.

Interestingly, the bulk state of the products also changed with the feed ratio, from viscous (HPG-C16(0)-PEG350(100)) to fragile (HCP-C16(100)-PEG350(0)). DSC measurements showed the glass transition temperature (T_g) of the polymer brushes increased from –21.0 to 18.2 °C when the R_{feed} changed from 25/75 to 100/0 (Table 3), which is quite coincident with the states of the products. Due to the crystalline side arms, the MHPBs with higher R_{feed} exhibited melting peak in the DSC measurements, and the corresponding melting-temperature (T_m) is also collected in Table 3.

3.4 Self-assembly of the miktoarms polymer brushes

The self-assembly properties of molecular brushes have attracted increasing interest. Micelles, tubes, and worm-like supramolecular structures were achieved by many research groups [6, 42–43]. Yan's group has done pioneering works on the self-assembly of amphiphilic core-shell hyperbranched polymers with homopolymer arms [34, 41]. But so far self-assembly of MHPBs was rarely studied as mentioned above [44]. This kind of complex macromolecules would promise more complex self-assembly behaviors. Herein, the self-assembly of the HPG-C16(36)-PEG350(64) which have approximately equal fraction of C16 arms and PEG350 arms were investigated by DLS and AFM measurements. The DLS column chart was shown in the Figure 5(a),

Table 3 Glass-transition temperatures (T_g) and melting points (T_m) of the series of HPG-*g*-C16/PEG350 measured by DSC

Samples	T_g (℃)	T_m (℃)
HPG-C16(100)-PEG(0)	18.2	80.8
HPG-C16(75)-PEG(25)	9.6	78.5
HPG-C16(50)-PEG(50)	1.0	58.0
HPG-C16(25)-PEG(75)	–21	—[a]

a) No melting point could be distinguished in the DSC curve.

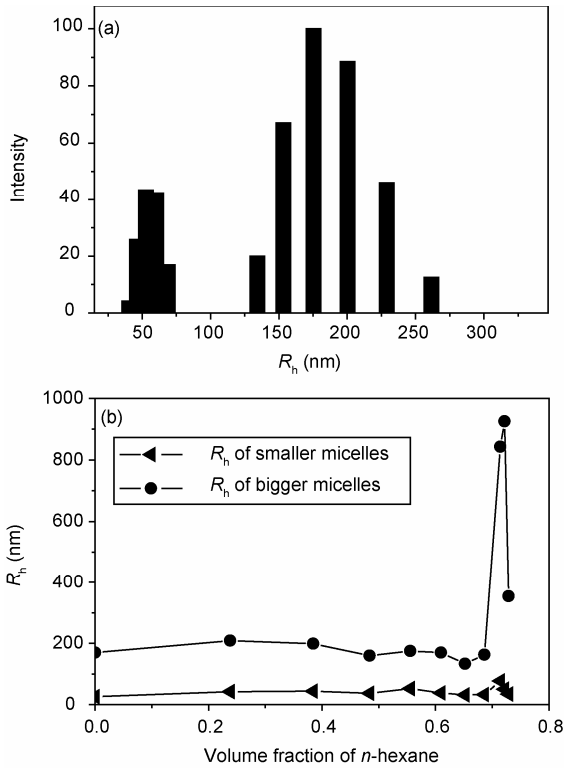

Figure 5 (a) DLS column chart of HPG-C16(36)-PEG350(64) when the volume fraction of *n*-hexane reached 0.56, in dichloromethane solution whose initial concentration was 1 mg/mL. (b) Change of hydrodynamics radius (R_h) with the adding of *n*-hexane for HPG-C16(36)-PEG350(64) in dichloromethane, and the initial concentration was 1 mg/mL.

in which the volume fraction of n-hexane was 0.56. According to the DLS data, it was found that two or three peaks can be recognized, and the highest intensity radius data points of each peak were selected to make the chart in Figure 5(b). As *n*-hexane was added into the CH_2Cl_2 solution of the brushes gradually, the smaller size particles always located around 40 nm, and the bigger size particles became larger and larger. At last the bigger particles reached as high as 1500 nm, indicating macro-aggregation happened (white turbidity appeared). During the hexane-addition process, samples were also made on mica substrates for AFM observations.

As shown in Figure 6, before any *n*-hexane was added,

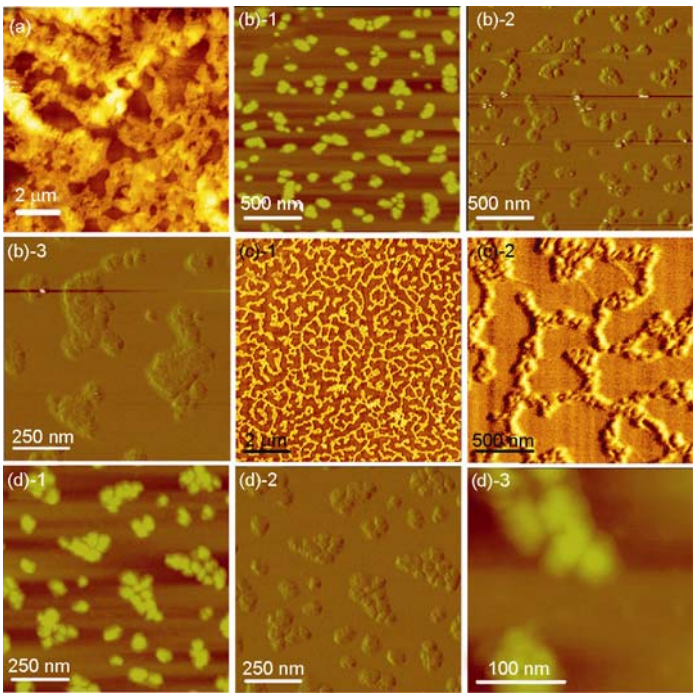

Figure 6 AFM images for HPG-C16(36)-PEG350(64) dissolved in dichloromethane after addition of *n*-hexane with the volume fraction 0 (a), 0.4 (b), 0.5 (c) and 0.72 (d). Among them, (b)-2, (b)-3, (c)-2, (d)-2 were phase images, and others are height images. The orginal concentration of HPG-C16(36)-PEG350(64) is 1 mg/mL.

the polymer existed in an amorphous state and no regular structure was detected (Figure 6(a)). When the volume fraction of *n*-hexane reached 0.4 of the solution, micelles with diameters around 100 nm were visible in the AFM image (Figure 6(b)). From the corresponding phase image, we can clearly recognized that a few smaller micelles aggregated into a bigger one. Some small micelles with sizes of about 50 nm can also be found, which we thought were unimolecular micelles of the miktoarm brushes [45–46]. In the DLS measurements described above, the particles with sizes of ~40 nm were also detected. This fact indicated that during all the self-assembly process, unimolecular micelles coexisted with the higher level assembly form (i.e. bigger micelles), as shown in Scheme 2.

When the volume fraction of *n*-hexane reached 0.5 of the solution, network-like fibers appeared in the AFM image (Figure 6(c)). From the phase image, we can identify that the fibers are composed of some spherical micelles, suggesting that small unimolecular micelles assembled into larger superstructures.

When the volume fraction of *n*-hexane reached 0.72 of the solution, again particles with diameters around 50 nm were visible in the AFM image (Figure 6(d)), indicating the formed fibers disassembled into unimolecular micelles.

This process showed hierarchical supramolecular self-assembly manners and can be divided into three stages, which could be illustrated by Scheme 2. In the shell of the polymer brushes, C16 arms are hydrophobic and the PEG350 arms are hydrophilic. The dichloromethane had been proved to be a good solvent for C16, PEG350 arms and alkyne modified HPG, the core of the polymer brush. But only C16 arms can be dissolved in *n*-hexane. Therefore at the beginning of the first stage, before any *n*-hexane was added, the polymer brushes were greatly extended in the solution, in which no special supramolecular structure could be detected. When a certain amount of *n*-hexane was adding into the solution, the PEG350 arms began to shrink, because *n*-hexane is poor solvent for both PEG350 arms and HPG core. As shown in Scheme 2, the core parts of the brushes aggregated together by a few unimolecules, and this can be observed from the AFM images. This was also coincident with the peaks around 200 nm in DLS results. At this state, unimolecular micelles were also found by AFM and DLS. In the second stage, when more *n*-hexane was added into the system, network-like fibers structure appeared. If we zoom in to investigate the network-like fibers by high resolution AFM, we could identify that the fibers was constructed by a lot of unimolecular micelles. It is quite possible that more and more core parts of the polymer brushes and the PEG350 arms aggregated together to avoid contacting with the poor solvent of hexane to maintain a lower energy level. But it is worthy to note that, in this case, the effect of solvent evaporation could not be neglected. Because such a big network should cause macroscopic phase separation, but in the DLS data no significant size increase was detected. So in our opinion, both self-assembly in solution and interfacial self-assembly on mica happened to form network-like fibers structure. Going to the third stage, when

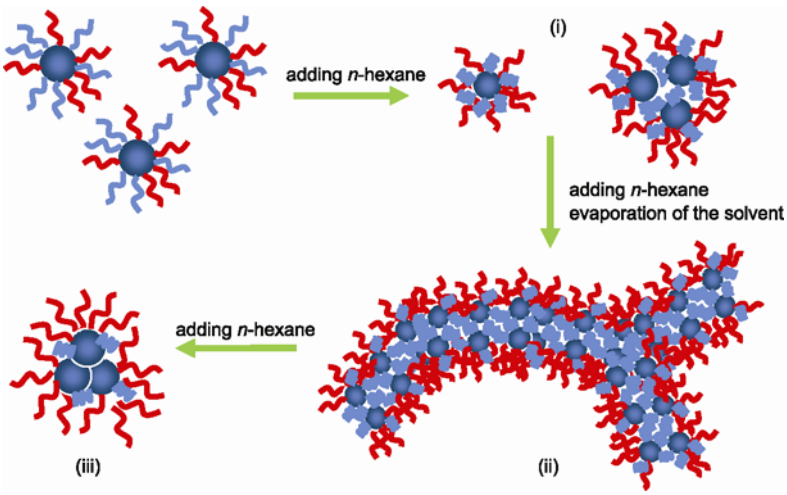

Scheme 2 Speculated mechanism for the self-assembly of HPG-C16(36)-PEG350(64) in three stages. (i) Unimolecular micelles and micelles formed by a few unimolecular micelles; (ii) network-like structures made from supramolecular fibres; (iii) micelles with extending C16 arms and more shrunken PEG350 arms.

the volume fraction of the *n*-hexane reached 0.6, the network-like fibers disappeared and assembled micelles and unimolecular micelles appeared again. This is probably because the solution had been diluted greatly. In this situation, C16 arms were extended but more PEG350 arms and the PEG core collapsed to lower the energy of the system. Compared with the micelles formed in the first stage, the micelles in the second stage have higher shrinking degree. At the end of the third stage, white turbidity appeared which indicated precipitation in macro-phase of the polymers had formed. However, the mechanism of the self-assembly of miktoarms polymer brushes are very complicated because the molecular structure was very complex. More research should be done to figure out the relation between the molecular structure and the supramolecular structure.

In all these stages, unimolecular micelles whose diameter ranged from 30 to 50 nm (measured from the AFM images) always existed and this agreed well with the DLS results. And the molecular brushes were visualized in the AFM images [46].

More AFM images corresponding to these three stages were listed in Figure 7 to support our speculation. Those AFM images were captured at other initial solution concentration (i.e. 0.5 mg/mL or 0.25 mg/mL) or solvent system (i.e. chloroform) in order to demonstrate that all those self-assembly manners were not occasional samples, but could be found in other cases. Unimolecular micelles with diameters about 50 nm (Figure 7(a)) corresponding to the stage 1 was obtained when the volume fraction of *n*-hexane reached 0.44, and the initial solution concentration was 0.25 mg/mL in dichloromethane. Network-like fibers (Figure 7(b)) corresponding to stage 2 was formed when the volume fraction of *n*-hexane reached 0.54, and the initial concentration was 0.5 mg/mL in chloroform. Examples for stage 3

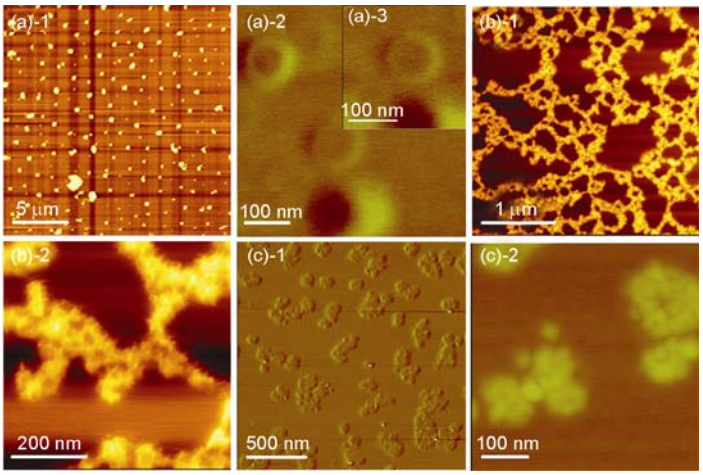

Figure 7 AFM images of HPG-C16(36)-PEG350(64) with the volume fraction of *n*-hexane being 0.44 (a), 0.54 (b) and 0.7 (c). The initial solution concentration was 0.25 (a), 0.5 (b) and 0.25 mg/mL (c) in dichloromethane, chloroform, and chloroform, respectively. Among them (a)-2, (a)-3 and (c)-1 are phase images.

can be found in Figure 7(c). The initial concentration of the system was 0.25 mg/mL in chloroform, and micelles could be obtained when the volume fraction of *n*–hexane was 0.7.

3.5 Dye loading of the miktoarms polymer brushes (HPG-*g*-C16/PEG350)

One of the most important attributes of HPs is their host-guest encapsulation to molecules such as dyes and drugs [47]. Herein, we also investigated the encapsulation property of the MHPBs primitively to show their possible intramolecular cavities. The encapsulation pictures were taken and shown in the Figure 8. From Figure 8, it can be observed by naked eyes that HPG-C16(100)-PEG350(0) was more capable of loading Congo red than HPG-C16(35)-PEG350(64) due to the higher polarity difference between core and shell for HPG-C16(100)- PEG350(0). The Figure 8 also indicated that the amphiphilic brushes solution in chloroform have the dye loading ability as well. It should be noted that, the flocculation at the interface between water and organic phase was the assembled polymer itself because of its amphiphilic property. The results indicated the potential use of this kind of heteroarm polymer brushes in drug delivery system, and more detailed work about the self-assembly of the dye loaded brushes will be done later.

4 Conclusions

Miktoarms polymer brushes with a hyperbranched polymer core and amphiphilic mixed arms were successfully synthesized by the parallel click grafting strategy. A series of HPG-*g*-C16/PEG350 was synthesized by grafting C16-N_3 and PEG350-N_3 onto HGP-alkyne. The arms ratio was controllable by just adjusting the feed fraction of C16 and-PEG350. The one-step grafting reaction could be finished within only two hours. The final products were easy to purify by precipitation in the proper precipitator. The high activity of the "click" reaction and the "soft" and "thin" arms made the efficiency in the grafting step near 100%. The high molecular weight of the core led to very large miktoarms polymer brushes whose molecular weights could exceed 200 kDa, making the molecular brushes visualized by AFM. The self-assembly properties of the amphiphilic polymer brushes were investigated by AFM and DLS. The supramolecular structures of the amphiphilic brushes went through such a process: micelles, network-like fibers and micelles again. The miktoarms polymer brushes also showed some ability of dye loading.

This synthesis approach proposed a new, simple and fast strategy to access the miktoarms polymer brushes, which may provide us an opportunity to understand the relationship between the structure of molecular brushes and their properties. But the potential applications of this kind of miktoarms polymer brushes in biology, solubilizer, drug delivery and catalysis are still need to be exploited [7, 8, 48–52].

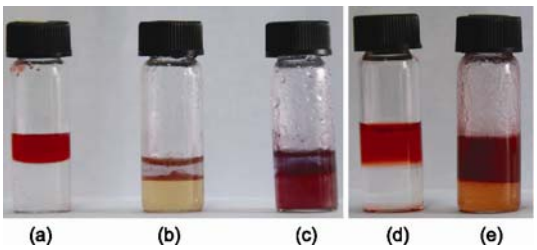

Figure 8 Photographs of Congo red water solution (upper layer) and dichloromethane (a), Congo red water solution and dichloromethane solubilized HPG-C16(36)-PEG350(64) (b), Congo red water solution and dichloromethane solubilized HPG-C16(100)-PEG350(0) (c), Congo red water solution and neat chloroform (d), and Congo red water solution and chloroform solubilized HPG-C16(36)-PEG350(64) (e).

This work was financially supported by the National Natural Science Foundation of China (50773038 & 20974093), National Basic Research Program of China (973 Program) (2007CB936000), the Fundamental Research Funds for the Central Universities (2009QNA4040), Qianjiang Talent Foundation of Zhejiang Province (2010R10021), and the Foundation for the Author of National Excellent Doctoral Dissertation of China (200527).

1 Zhang MF, Muller AHE. Cylindrical polymer brushes. *J Polym Sci, Part A: Polym Chem*, 2005, 43(16): 3461–3481
2 Sheiko SS, Sumerlin BS, Matyjaszewski K. Cylindrical molecular brushes: Synthesis, characterization, and properties. *Prog Polym Sci*, 2008, 33(7): 759–785
3 Gao C, Zheng X. Facile synthesis and self-assembly of multihetero-arm hyperbranched polymer brushes. *Soft Mater*, 2009, 5(23): 4788–4796
4 Knischka R, Lutz PJ, Sunder A, Mulhaupt R, Frey H. Functional poly(ethylene oxide) multiarm star polymers: Core-first synthesis using hyperbranched polyglycerol initiators. *Macromolecules*, 2000, 33(2): 315–320
5 Burgath A, Sunder A, Neuner I, Mulhaupt R, Frey H. Multi-arm star block copolymers based on epsilon-caprolactone with hyperbranched polyglycerol core. *Macromol Chem Phys*, 2000, 201(7): 792–797
6 Wan DC, Fu Q, Huang JL. Synthesis of amphiphilic hyperbranched polyglycerol polymers and their application as template for size control of gold nanoparticles. *J Appl Polym Sci*, 2006, 101(1): 509–514
7 Liu HJ, Chen Y, Shen Z, Frey H. Multiarm star polyglycerol-block-poly(HEMA) as a versatile precursor for the preparation of micellar nanocapsules with different properties. *React Funct Polym*, 2007, 67(2): 156–164
8 Turk H, Shukla A, Rodrigues PCA, Rehage H, Haag R. Water-soluble dendritic core-shell-type architectures based on polyglycerol for solubilization of hydrophobic drugs. *Chem Eur J*, 2007, 13(15): 4187–4196
9 Wan DC, Yuan JJ, Pu HT. Macromolecular nanocapsule derived from hyperbranched polyethylenimine (HPEI): Mechanism of guest encapsulation versus molecular parameters. *Macromolecules*, 2009, 42(5): 1533–1540
10 Xu SJ, Luo Y, Graeser R, Warnecke A, Kratz F, Hauff P, Licha K, Haag R. Development of pH-responsive core-shell nanocarriers for delivery of therapeutic and diagnostic agents. *Bioorg Med Chem Lett*, 2009, 19(3): 1030–1034
11 Xie MR, Dang JY, Shi JX, Han HJ, Song CM, Huang W, Zhang YQ. Synthesis and self-assembly of well-defined polymer brushes with high grafting density of hydrophobic poly(epsilon-caprolactone) and hydrophilic poly(2-(dimethylamino)ethyl methacrylate) side chains. *Acta Chim Sinica*, 2009, 67(8): 869–874

12 Xie MR, Dang JY, Han HJ, Wang WZ, Liu JW, He XH, Zhang YQ. Well-defined brush copolymers with high grafting density of amphiphilic side chains by combination of ROP, ROMP, and ATRP. *Macromolecules*, 2008, 41(23): 9004–9010

13 Li ZY, Li P, Huang JL. Synthesis of amphiphilic copolymer brushes: Poly(ethylene oxide)-*graft*-polystyrene. *J Polym Sci, Part A: Polym Chem*, 2006, 44(15): 4361–4371

14 Li CH, Ge ZS, Fang J, Liu SY. Synthesis and self-assembly of coil-rod double hydrophilic diblock copolymer with dually responsive asymmetric centipede-shaped polymer brush as the rod segment. *Macromolecules*, 2009, 42(8): 2916–2924

15 Huang Y, Liu Q, Zhou X, Perrier Sb, Zhao Y. Synthesis of silica particles grafted with well-defined living polymeric chains by combination of raft polymerization and coupling reaction. *Macromolecules*, 2009, 42(15): 5509–5517

16 Li YG, Zhang YQ, Yang D, Li YJ, Hu JH, Feng C, Zhai SJ, Lu GL, Huang XY. PAA-*g*-PPO amphiphilic graft copolymer: Synthesis and diverse micellar morphologies. *Macromolecules*, 2010, 43(1): 262–270

17 Zhang YQ, Shen Z, Yang D, Feng C, Hu JH, Lu GL, Huang XY. Convenient synthesis of PtBA-*g*-PMA well-defined graft copolymer with tunable grafting density. *Macromolecules*, 2010, 43(1): 117–125

18 Liu C, Zhang Y, Huang JL. Well-defined star polymers with mixed-arms by sequential polymerization of atom transfer radical polymerization and reverse addition-fragmentation chain transfer on a hyperbranched polyglycerol core. *Macromolecules*, 2008, 41(2): 325–331

19 Gao HF, Matyjaszewski K. Synthesis of low-polydispersity miktoarm star copolymers via a simple "Arm-First" method: Macromonomers as arm precursors. *Macromolecules*, 2008, 41(12): 4250–4257

20 Gao HF, Matyjaszewski K. Synthesis of molecular brushes by "grafting onto" method: Combination of ATRP and click reactions. *J Am Chem Soc*, 2007, 129(20): 6633–6639

21 Gao HF, Matyjaszewski K. Synthesis of star polymers by a combination of ATRP and the "click" coupling method. *Macromolecules*, 2006, 39(15): 4960–4965

22 Zhong L, Zhou YF, Yan DY, Pan CY. Synthesis of a multi alternating-arm-containing dendritic star copolymer by RAFT and cationic ring-opening polymerization. *Macromol Rapid Comm*, 2008, 29(16): 1385–1391

23 Killops KL, Campos LM, Hawker CJ. Robust, efficient, and orthogonal synthesis of dendrimers via thiol-ene “click” chemistry. *J Am Chem Soc*, 2008, 130(15): 5062–5064

24 Wu J, He H, Gao C. Sliding supramolecular polymer brushes with tunable amphiphilicity: One-step parallel click synthesis and self-assembly. *Macromolecules*, 2010, 43(17): 7139–7146

25 Gao C, Yan D. Hyperbranched polymers: From synthesis to applications. *Prog Polym Sci*, 2004, 29(3): 183–275

26 Zhou L, Gao C, Xu WJ. Efficient grafting of hyperbranched polyglycerol from hydroxyl-functionalized multiwalled carbon nanotubes by surface-initiated anionic ring-opening polymerization. *Macromol Chem Phys*, 2009, 210(12): 1011–1018

27 Zhou L, Gao C, Xu WJ, Wang X, Xu YH. Enhanced biocompatibility and biostability of CdTe quantum dots by facile surface-initiated dendritic polymerization. *Biomacromolecules*, 2009, 10(7): 1865–1874

28 Calderon M, Quadir MA, Sharma SK, Haag R. Dendritic polyglycerols for biomedical applications. *Adv Mater*, 2010, 22(2): 190–218

29 Kainthan RK, Muliawan EB, Hatzikiriakos SG, Brooks DE. Synthesis, characterization, and viscoelastic properties of high molecular weight hyperbranched polyglycerols. *Macromolecules*, 2006, 39(22): 7708–7717

30 Wilms D, Stiriba SE, Frey H. Hyperbranched polyglycerols: From the controlled synthesis of biocompatible polyether polyols to multipurpose applications. *Accounts Chem Res*, 2010, 43(1): 129–141

31 Kolb HC, Finn MG, Sharpless KB. Click chemistry: Diverse chemical function from a few good reactions. *Angew Chem Int Ed*, 2001, 40(11): 2004–2021

32 Lutz JF. 1,3-Dipolar cycloadditions of azides and alkynes: A universal ligation tool in polymer and materials science. *Angew Chem Int Ed*, 2007, 46(7): 1018–1025

33 Lee S, Spencer ND. Materials science - Sweet, hairy, soft, and slippery. *Science*, 2008, 319(5863): 575-–576

34 Jia ZF, Zhou YF, Yan DY. Amphiphilic star-block copolymers based on a hyperbranched core: Synthesis and supramolecular self-assembly. *J Polym Sci, Part A: Polym Chem*, 2005, 43(24): 6534–6544

35 Zhou YF, Yan DY. Supramolecular self-assembly of amphiphilic hyperbranched polymers at all scales and dimensions: Progress, characteristics and perspectives. *Chem Commun*, 2009, 10: 1172–1188

36 Adeli M, Haag R. Multiarm star nanocarriers containing a poly(ethylene imine) core and polylactide arms. *J Polym Sci, Part A: Polym Chem*, 2006, 44(19): 5740–5749

37 Yan DY, Zhou YF, Hou J. Supramolecular self-assembly of macroscopic tubes. *Science*, 2004, 303(5654): 65–67

38 Ranganathan K, Deng R, Kainthan RK, Wu C, Brooks DE, Kizhakkedathu JN. Synthesis of thermoresponsive mixed arm star polymers by combination of RAFT and ATRP from a multifunctional core and its self-assembly in water. *Macromolecules*, 2008, 41(12): 4226–4234

39 Gao C, He H, Zhou L, Zheng X, Zhang Y. Scalable functional group engineering of carbon nanotubes by improved one-step nitrene chemistry. *Chem Mater*, 2008, 21(2): 360–370

40 Zhang Y, He H, Gao C. Clickable macroinitiator strategy to build amphiphilic polymer brushes on carbon nanotubes. *Macromolecules*, 2008, 41(24): 9581–9594

41 Hong HY, Mai YY, Zhou YF, Yan DY, Chen Y. Synthesis and supramolecular self-assembly of thermosensitive amphiphilic star copolymers based on a hyperbranched polyether core. *J Polym Sci, Part A: Polym Chem*, 2008, 46(2): 668–681

42 Runge MB, Lipscomb CE, Ditzler LR, Mahanthappa MK, Tivanski AV, Bowden NB. Investigation of the assembly of comb block copolymers in the solid state. *Macromolecules*, 2008, 41(20): 7687–7694

43 Hermans TM, Broeren MAC, Gomopoulos N, van der Schoot P, van Genderen MHP, Sommerdijk N, Fytas G, Meijer EW. Self-assembly of soft nanoparticles with tunable patchiness. *Nat Nanotechnol*, 2009, 4(11): 721–726

44 Zou JH, Ye XD, Shi WF. Crosslinkable vesicles self-assembled by amphiphilic hyperbranched polyester. *Macromol Rapid Commun*, 2005, 26(21): 1741–1745

45 Schappacher M, Deffieux A. Atomic force microscopy imaging and dilute solution properties of cyclic and linear polystyrene combs. *J Am Chem Soc*, 2008, 130(44): 14684–14689

46 Hans M, Mourran A, Henke A, Keul H, Moeller M. Synthesis, characterization, and visualization of high-molecular-weight poly(glycidol-*graft*-epsilon-caprolactone) starlike polymers. *Macromolecules*, 2009, 42(4): 1031–1036

47 Liu C, Gao C, Yan D. Honeycomb-patterned photoluminescent films fabricated by self-assembly of hyperbranched polymers13. *Angew Chem Int Ed*, 2007, 46(22): 4128–4131

48 Kramer M, Stumbe JF, Turk H, Krause S, Komp A, Delineau L Prokhorova S, Kautz H, Haag R. pH-Responsive molecular nanocarriers based on dendritic core-shell architectures. *Angew Chem Int Ed*, 2002, 41(22): 4252–4256

49 Wan DC, FuQ, Huang JL. Synthesis of a thermoresponsive shell-crosslinked 3-layer onion-like polymer particle with a hyperbranched polyglycerol core. *J Polym Sci, Part A: Polym Chem*, 2005, 43(22): 5652–5660

50 Elmer S L, Man S, Zimmerman S C. Synthesis of polyglycerol, porphyrin-cored dendrimers using click chemistry. *Eur J Org Chem*, 2008, 22: 3845–3851

51 Kainthan RK, Mugabe C, Burt HM, Brooks DE. Unimolecular micelles based on hydrophobically derivatized hyperbranched polyglycerols: Ligand binding properties. *Biomacromolecules*, 2008, 9(3): 886–895

52 Wang SW, Zhang B, Ai P, Zhu M, Wang W, Sa ZP, Ma LN, Li YP. Chemoenzymatic synthesis amphiphilic H-shaped copolymer and its self-assembly behavior. *Sci China Ser B*, 2009, 39(6): 518–524